Molecular Biology Reports (2025) 52:482
https://doi.org/10.1007/s11033-025-10585-1

ORIGINAL ARTICLE

Synergistic effects and mechanism of recombinant viral vector-mediated STAT1 overexpression and STAT3 silencing on glioma U251 apoptosis

Xin-Long Hu[1] · Hong Li[2] · Guo-Dong Zhang[3] · Chao Lin[4] · Ping Huang[5] · Xiu-Feng Chen[1] · Fang Wan[6] · Chang-Wu Dou[5] · Hai-Tao Ju[5]

Received: 16 October 2024 / Accepted: 8 May 2025

Abstract

Background In the present study, the synergistic effects and mechanism of recombinant viral vector-mediated co-expression plasmids stat1 and stat3-siRNA on glioma were investigated in vivo and in vitro.

Methods Co-expression plasmids for stat1/stat3-siRNA were constructed and packaged into lentivirus and adenovirus for cell and animal experiments. Real-time PCR and Western blot analyses were used to detect the expression of STAT1 and STAT3 at gene and protein levels in U251 cells. CCK-8, TUNEL, flow cytometry, and cell scratching assays were performed to detect the therapeutic effect of the co-expression plasmid stat1/stat3-siRNA on glioma in vitro. U251 glioma cells were injected into nude mice to observe therapeutic effect of stat1/stat3-siRNA.Transcriptome sequencing was utilized to further explore the possible mechanism.

Results Treatment of glioma cells and xenograft animal model with the co-expression plasmid stat1/stat3-siRNA led to a significant increase in STAT1 and a marked decrease in STAT3 expression at both mRNA and protein expression levels. Compared to the single-gene stat1 and stat3-siRNA groups, stat1/stat3-siRNA group demonstrated a more pronounced promoting apoptosis of U251, but cell viability and migration, as well as reduced tumor growth in nude mice were not significant. Transcriptome sequencing results indicated that the modulation of multiple nodes within the FOXO signaling pathway may represent the main mechanism by which co-expression of lenti-stat1/stat3-SiRNA induces U251 cell apoptosis.

Conclusions The co-expression plasmid stat1/stat3-siRNA significantly induces apoptosis more effectively than individual stat1 and stat3-siRNA constructs. The potential mechanism involves the alternation of multiple nodes in the FOXO signaling pathway.

Keywords Glioma · STAT1 · STAT3 · Gene therapy · Viral vector

Hai-Tao Ju and Chang-Wu Dou have contributed equally to this paper.

✉ Chang-Wu Dou
Douchangwu@sina.com.cn

✉ Hai-Tao Ju
1573694403@qq.com

[1] Department of General Surgery, Aerospace Center Hospital, Beijing 100049, China

[2] Present Address: Department of Radiation Oncology, Peking University Cancer Hospital (Inner Mongolia Campus) & Afliated Cancer Hospital of Inner Mongolia Medical University, Hohhot 010020, Inner Mongolia Autonomous Region, China

[3] Department of Neurosurgery, Affiliated Hospital of Chifeng University, Chifeng 024000, Inner Mongolia Autonomous Region, China

[4] Department of General Surgery, Beijing Nuclear Industry Hospital, Beijing 100045, China

[5] Department of Neurosurgery, Affiliated Hospital of Inner Mongolia Medical University, No.1, Tongdao North Road, Hohhot, Inner Mongolia Autonomous Region, China

[6] School of Life Sciences, Inner Mongolia Agricultural University, Hohhot 010000, Inner Mongolia Autonomous Region, China

Published online: 22 May 2025

Introduction

Glioma is one of the most common malignant tumors in the central nervous system (CNS) [1]. Currently, the overall treatment outcomes are unsatisfactory. In recent decades, gene therapy has exhibited great potential to enhance existing therapeutic strategies for glioma [2, 3]. Signal transducer and activator of transcription (STAT) is a cytoplasmic transcription factor that functions through JAK/STAT pathway. Under normal physiological conditions, the JAK/STAT pathway is involved in the regulation of cell proliferation, differentiation, apoptosis, immune response, and expression of various essential biological function genes. However, dysregulation of this pathway can lead to the constitutive activation of STAT proteins, driving cell proliferation, inflammation, and uncontrolled immune response [4–6].

Currently, STAT1 is recognized for its role in growth arrest and apoptosis, acting as a tumor-dependent suppressor [7, 8]. In contrast, STAT3 is implicated not only in the proliferation, invasion, and migration of cancer cells, but also in the tumor formation and progression. It facilitates the epithelial-mesenchymal transition phenotype of cancer cells, regulates the tumor microenvironment, and promotes the self-renewal of tumor stem cells [9]. Ju et al. [10] detected the expression of STAT1 in glioma tissue and normal brain tissue by immunohistochemistry and confirmed that STAT1 is highly expressed in human normal brain tissue, but its expression is significantly reduced or absent in human glioma tissue. They also confirmed that STAT1 had an inhibitory effect on glioma in vivo and in vitro. However, STAT3 is widely expressed in gliomas, but is absent in peritumoral or normal tissues [11]. Other studies have shown that STAT3 and its downstream genes, such as cyclin D1, c-myc, Bcl-2, BCL XL, and VEGF, play critical roles in the initiation and progression of various tumors, including glioma [12] and colorectal cancer [13].

In summary, STAT1 is generally considered to be a tumor-dependent suppressor, while STAT3 is defined as a carcinogenic gene. STAT3 inhibitor [14] has shown therapeutic potential in the treatment of glioma. Additionally, it is crucial to choose a reasonable delivery vector for gene therapy. Therefore, we constructed the co-expression plasmid stat1/stat3-SiRNA to upregulate the expression of STAT1 and downregulate the expression of STAT3, which was subsequently packaged into lentivirus and adenovirus. Furthermore, we investigated its effect on glioma and elucidated the underlying molecular mechanism through in vivo and in vitro experiments.

Materials and methods

Cell lines, plasmids and viruses

The U251 glioma cell line was obtained from the Laboratory of Molecular pharmacology at Inner Mongolia Agricultural University. The construction, packaging, and sequencing identification of stat1, stat3-siRNA, co-expression stat3-siRNA-stat1 plasmid, and its recombinant lentiviral and adenoviral vectors were performed by the Shanghai Jikai Gene Company. A detailed schematic representation of the vectors used in our study is provided in supplemental materials Figure S1.

Cell culture and lentivirus infection

The human glioma cell line U251 was cultured in RMPI-1640 medium with 10% fetal bovine serum at 37 °C, 5% CO_2 for 24 h. Based on the optimal multiplicity of infection (MOI) value (30) of each group (determined by the pre-experimental results), combined with the titer of each group of lentivirus, and using the formula: virus volume = (MOI × cell number)/virus titer, we calculated the optimal amount of virus use and added the virus for infection. Approximately 72 h post-infection, fluorescence was observed under the microscope to determine the infection efficiency, and subsequent experiments were carried out. The following cell experiments were categorized into the mock group (blank control group), lenti con group (negative control lentivirus), lenti stat1 group (overexpression of stat1 lentivirus), lenti stat3 siRNA group (knockout of stat3 lentivirus), and lenti stat1/stat3 siRNA group (overexpression of stat1 and knockout of stat3 lentivirus).

Cell morphology and infection efficiency assessment

The morphology of U251 cells was observed using a microscope 72 h after infection with recombinant lentivirus and mock group U251 Cell. Each lentivirus group carries GFP as the reporter gene. The quantity and intensity of GFP can be observed directly by microscope and photographed. Additionally, the infection efficiency was assessed by flow cytometry.

Quantitative RT-PCR

Total RNA was extracted using the total RNA rapid extraction kit provided by Feijie biological company. Following extraction, the total RNA was reverse transcribed into cDNA using the reverse transcription kit of Takara

company (Dalian, China). According to the primers corresponding to cDNA sequence of STAT1 and STAT3 genes were designed and synthesized by Takara company based on sequences available in the GenBank database. For STAT1, the forward primer sequence is 5′-GCTGGCACC AGAACGAATGA-3′, and the reverse primer sequence is 5′-TACCAAACCAGGCTGGCACA-3′. For STAT3, the forward primer sequence is 5′-ACCAGCAGTATAGCC GCTTCC-3′, and the reverse primer sequence is 5′-CCA TTGGCTTCTCAAGATACC-3′.

The PCR mixture includes SYBR premier ex Taq II (TLI RNaseH plus) (2×) (12.5μL), primer f (10μm) (1μL), primer R (10μm) (1μL), cDNA (2μL), dH2O (8.5μL). PCR amplification conditions: 95 °C 30 s, 95 °C 5 s, 60 °C 30 s, 30 cycles. The change in fluorescence signal was monitored using real-time PCR. At the end of the reaction, the results of STAT1 and STAT3 mRNA relative expression were analyzed and displayed automatically by computer, and calculated by 2-ΔΔ CT method. β-actin served as the internal reference to ensure the normal expression of the target gene. The experiment was conducted in triplicate and statistical analysis was performed using the t-test.

Western blotting

Total protein was extracted using the RIPA cell lysate kit of Beijing Suo Lai Bao Technology Co.; Ltd. The protein concentration was determined using the BCA assay. Equivalent protein samples (40 ug) were subjected to a heat treatment in a metal bath at 95 °C 5min, then cooled to room temperature, and centrifuged at 12,000 rpm for 3 min. The supernatant was separated on 8% twelve alkyl sulfate–polyacrylamide gel (SDS-PAGE) and transferred to the nitrocellulose membrane (NC membrane). The NC membrane was incubated in TBST and subsequently placed in a sealing box containing 5% skim milk powder. It was agitated at 100 RPM at room temperature for 3 h to block non-specific binding. The dilution ratio of the first antibody: 1:500 for STAT1 antibody, 1:500 for STAT3 antibody, and 1:10,000 for β-actin internal reference. After fully mixing, the first antibody was placed in a low-temperature shaker for 60 RPM, 4 °C overnight.

Following incubation, the membrane was washed with TBST on the shaker at 120 RPM for 5 min each time. Then we added the appropriate amount of fluorescent secondary antibody (dilution ratio: 1:10,000) to mix well and avoid light. The membrane was then incubated at room temperature on a shaking table at 100 RPM for 1.5 h. After the membrane was washed 5 times in the same way and was scanned using a Li-Cor scanner at the appropriate wavelength for the secondary antibody. Band intensity was quantified using the ImageJ software for quantitative analysis.

Cell viability

Cell viability for each group was measured using the Cell Counting Kit-8 (CCK-8) method at 36 h and 72 h after infection with lentivirus. U251 cells in the logarithmic growth phase were prepared as suspension, with 5000 cells seeded per well in 96 well plates. After a 24-h pre-culture, the virus load was calculated according to MOI = 30 and added to the well plates for infection, the cell status was maintained in the middle of the infection, and 10μl CCK-8 solution was added into each well at 36 and 72 h, respectively. After incubation for 2 h, the absorbance at 450 nm was measured by enzyme labeling instrument. According to the formula: cell survival rate% = (ODtreated—ODblank)/(ODcontrol -ODblank) × 100%, the survival rates of each group at 36 and 72 h were calculated, and the results were presented in histogram format.

Apoptotic assay

The U251 cells in each group were digested and collected by trypsin without EDTA and resuspended in phosphate-buffered saline (PBS). The cells were centrifuged at 2000 RPM for 5 min, the supernatant was discarded. 500 μL binding buffer cells were added. Annexin v-APC was added to the mixture followed by the addition of 5 μL of propidium iodide (PI). After incubation at room temperature and in dark for 15 min, the apoptosis rate of each group was measured using a flow cytometer.

Cell scratch assay

Using 1ml syringe needle tip, parallel lines were drawn on the back of 12-hole plate, with an interval of about 0.5–1.0 cm. U251 cells were treated as suspensions and seeded in 12 well plates with 2×10^5 cells/well. After overnight culture in media depleted with serum, lentiviruses were added to each well according to MOI (30) to initiate infection. Then, the cells were scratched with a pipette gun perpendicular to the transverse line on the back. Different visual fields were taken and recorded as D0. After 12 h, the cells were replaced with a complete medium for further culture. At 36 and 72 h, the same visual field as D0 was taken and recorded as D36 and D72, respectively. The Age J system was used to analyze the data of cell scratch area (Δs) and draws the histogram.

Tumor growth in vivo

A suspension of the U251 glioma cells was injected into the armpit of the right forelimb of 4–6 weeks old BALB/c female nude mice (SPF grade), Tumor formation was observed after 2 weeks (the average tumor volume was 80-100mm^3, and the bodyweight was 18–20 g). The mice

were housed in IVC system rat house, room temperature is stable 24–27 °C, relative humidity is 50%. Litter and drinking water were replaced in a sterile fume hood every other day. All litter, feed, drinking water and squirrel cages underwent high-pressure sterilization. Animal breeding and experimentation were carried out in strict accordance with the requirements of the "Regulations on the Administration of Animal Experiments" of the People's Republic of China.

A total of 36 nude mice were randomly divided into 6 groups (n = 6 each): ①Ad-stat1②NCAd-stat1③Ad-stat3-siRNA④NCAd-stat3-siRNA⑤Ad-stat1/stat3-siRNA⑥NCAd-stat1/stat3-siRNA control group. Each group received intratumoral multipoint injections, with each dose of $2x10^9$pfu/50μl corresponding to the amount of adenovirus, the NCAd-stat1/stat3-siRNA group 50μL /mouse, once every other day, a total of 5 injections. The activity status, food intake and water intake, and weight changes of each group of nude mice were monitored daily. The long diameter (a) and short diameter (b) of the transplanted tumor were measured before and after the administration. According to the formula ($V = axb^2/2$) the tumor volume-time curve was subsequently plotted. One week after the final treatment, the nude mice were euthanized via cervical dislocation. The tumors were excised weighed and photographed. Half of the tumors in each group was used for HE staining, immunohistochemical detection, and TUNEL detection, and the other half was placed in a liquid nitrogen tank for extraction of total protein and RNA to detect the expression of stat1 and stat3 at the protein and gene level.

Transcriptome sequencing analysis

After extracting total RNA from each group of U251 cells 72 h post-infection with lentivirus, a library was constructed after total RNA sample detection. The library construction process included mRNA enrichment, double-stranded cDNA synthesis, end repair plus A and adaptor, fragment selection, and PCR amplification. Qubit 2.0 fluorometer was used for preliminary quantification, diluted to 1.5 ng/uL, and then Agilent 2100 Bioanalyzer was used to detect the insert size of the library. Once the library inspectionwas qualified, the different libraries were pooled according to the requirements of effective concentration and target off-line data volume. Sequencing was conducted on the Illumina hisep 3000 platforms, and the sequenced results are analyzed using tophat2 software.

Statistical analysis

All measurement data are expressed as mean ± standard deviation (SD). All the data are normally distributed. t-test was performed to analyze differences between two groups. One-way ANOVA was used to analyze intergroup differences with a Bonferroni multiple comparison post-test. All experiments were repeated at least 3 times. $P < 0.05$ was considered statistically significant.

Results

Verification of the U251 cells infection by recombinant lentivirus

In this experiment, three recombinant lentiviral vectors (lenti-stat1, lenti-stat3-siRNA, and lenti-stat1/stat3-siRNA) were constructed. These vectors were designed to overexpress STAT1, knock-out STAT3, and co-express lentiviral vectors that express these two genes simultaneously. Under the fluorescence microscope, green fluorescent protein expression was observed in lenti-con, lenti-stat1, lenti-stat3-siRNA, lenti-stat1/stat3-siRNA groups, but no green fluorescence was found in the mock group (Fig. 1A). According to results shown by flow cytometry, the infection rates of the groups mentioned above were 90.83 ± 0.04%, 81.49 ± 0.31%, 80.11 ± 0.56% and 77.41 ± 0.38%, respectively (Fig. 1B).

After these lentiviral vectors were transduced into U251 cells, Real-time PCR and Western blot were utilized to determine mRNA and protein levels of these two genes. The results showed that after transfection with lenti-stat3-siRNA and lenti-stat1/stat3-siRNA, compared to the Mock group, STAT3 was significantly down-regulated in mRNA and protein levels. And after infected with lenti-stat1 or lenti -stat1/stat3-siRNA, STAT1 was significantly up-regulated in mRNA and protein levels compared with the Mock group (Fig. 1C, D).

Effects of recombinant lentiviruses on viability and apoptosis in U251 Cell

In this study, untreated U251 cells and U251 cells treated with various recombinant lentivirus were selected to evaluate the growth of U251 cells and the synergistic effect of the STAT1 gene and STAT3 siRNA gene on glioma. The results demonstrated that U251 cells in both the mock control and lenti-con control groups maintained normal morphology, exhibiting typical growth patterns, uniform cellular distribution, and well-defined cellular architecture. However, U251 cells treated with lenti-stat1, lenti-stat3-siRNA, and lenti-stat1/stat3-siRNA showed cytopathological changes in varying degrees, including inhibited growth, scattered distribution, and the increase of cell debris. Comparing with lenti-stat1 and lenti-stat3-siRNA, lenti-stat1/stat3-iRNNA has obvious growth inhibition and killing effects on U251 cells but the difference is not significant ($P > 0.05$) (Fig. 2A).

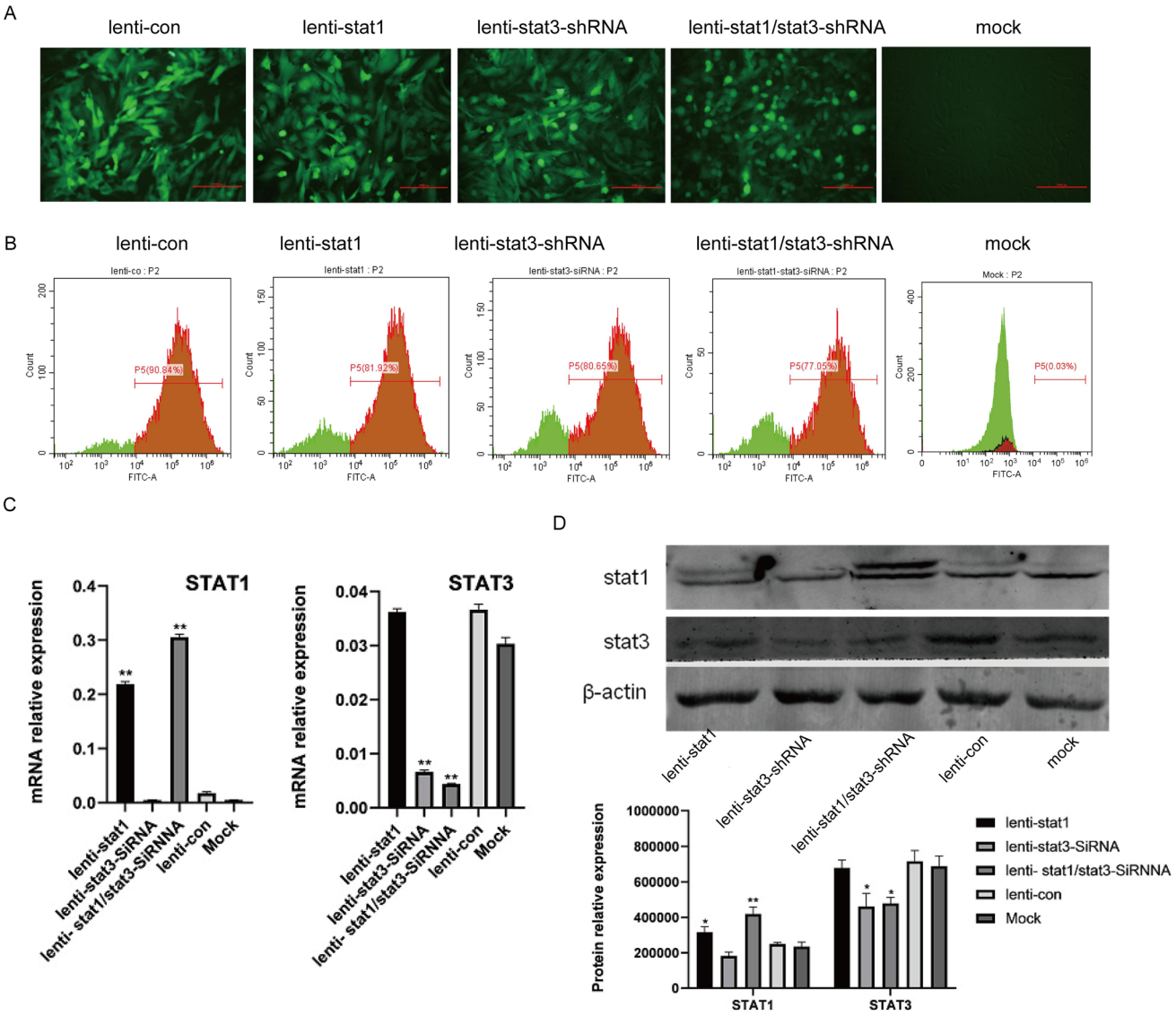

Fig. 1 Verification of the U251 cells infection by recombinant lentivirus. **A** Infection efficiency was verified by immunofluorescence. U251 cells were infected with lenti-con, lenti-stat1, lenti-stat3-shRNA, lenti-stat1/stat3-shRNA and mock. **B** Infection efficiency was verified by flow cytometry. **C** and **D** The relative expression of stat1 and stat3 mRNA and proteins after each recombinant lentivirus infects U251 cells, Recombinant lentivirus include lenti-stat1, lenti-stat3-shRNA and lenti-stat1/stat3-shRNA, lenti-con and Mock groups. One-way ANOVA was used to analyze intergroup differences with a Bonferroni multiple comparison post-test. n = 3, $*P < 0.05$, $**P < 0.01$vs lenti-con

CCK-8 results showed that compared with the mock group, the survival rates of U251 cells after transfection of lenti-stat1, lenti-stat3-siRNA, and lenti-stat1/stat3-siRNA were significantly reduced ($P < 0.01$). However, compared with lenti-stat1 or lenti-stat3-siRNA, the survival rate of U251 cells decreased slightly after lenti-stat1/stat3-siRNA transfection ($P > 0.05$) (Fig. 2B).

Apoptotic results showed that compared with the mock group, lenti-stat1, lenti-stat3-siRNA, and lenti-stat1/stat3-siRNA all showed significant effect to induce apoptosis ($p < 0.05$). Compared with lenti-stat1 and lenti-stat3-siRNA, the apoptosis of U251 cells infected by lenti-stat1/stat3-siRNA was more obvious. The apoptosis rates of mock, lenti-con, lenti-stat1, lenti-stat3-siRNA, and lenti-stat1/stat3-siRNA were respectively: 8.91 ± 1.01%, 9.01 ± 3.33, 17.67 ± 4.29%, 17.26 ± 2.60% and 26.02 ± 4.21% (Fig. 2C). The result shows that lenti-stat1, lenti-stat3-siRNA, and lenti-stat1/stat3-siRNA can all induce U251 cell apoptosis, and lenti-stat1/stat3-siRNA can induce U251 cell apoptosis with a more prominent effect (Fig. 2D).

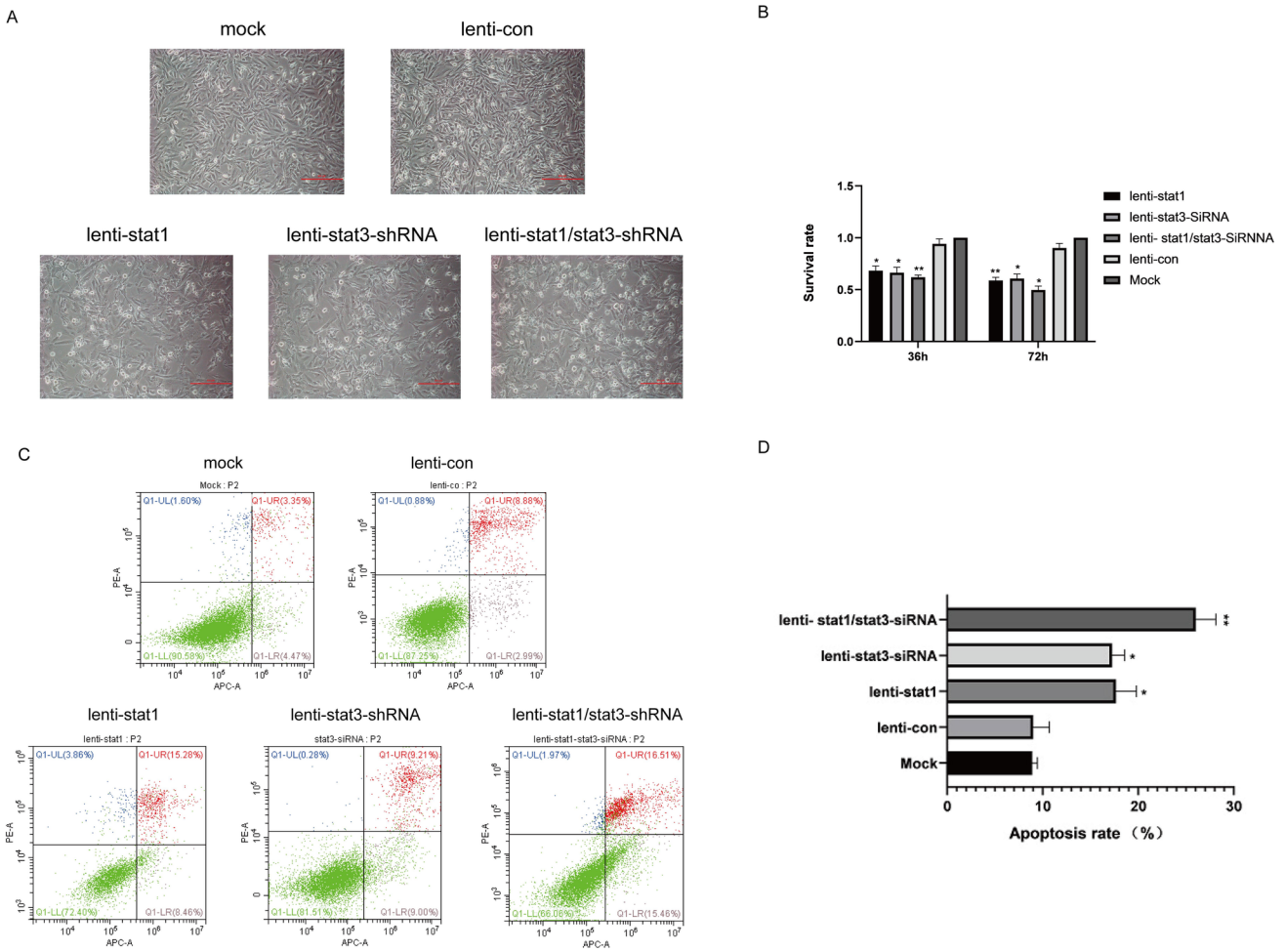

Fig. 2 Effects of recombinant lentiviruses on viability and apoptosis in U251 Cells. **A** Morphological changes of U251 cells after infection with mock, lenti-con, lenti-stat1, lenti-stat3-shRNA, and lenti-stat1/stat3-shRNA. Cell morphology was observed under microscope after incubation 72 h. **B** Survival rate of U251 cells detected by the CCK-8 method at 36 h and 72 h after infection. **C** and **D** Apoptosis rate of U251 cells after infection with mock, lenti-con, lenti-stat1, lenti-stat3-shRNA, and lenti-stat1/stat3-shRNA detected by the AnnexinV/PI double staining method at 72 h after infection. One-way ANOVA was used to analyze intergroup differences with a Bonferroni multiple comparison post-test. n = 3, * $P < 0.05$, ** $P < 0.01$ vs lenti-con

The effect of various recombinant lentiviruses on the migration of U251 cells

The cell scratch assay was employed to analyze the migration ability of U251 cells infected with recombinant lentivirus. The results showed that the migration ability of U251 cells infected with lenti-stat1, lenti-stat3-siRNA, and lenti-stat1/stat3-siRNA was significantly reduced compared to the mock group ($p < 0.01$) (Fig. 3A, B). Furthermore, U251 cells infected with lenti-stat1/stat3-siRNA exhibited a lower migration capability than those infected with lenti-stat1 or lenti-stat3-siRNA. The results indicate that lenti-stat1, lenti-stat3-siRNA, and lenti-stat1/stat3-siRNA inhibit the migration ability of U251 cells, but there are no differences between individual treatments and combined stat1-stat3 siRNA group (Fig. 3A, B).

Effects of recombinant adenovirus Ad-stat1/stat3-siRNA on tumor growth in vivo

Tumors were excised from the nude mice and volumes were measured. The tumor volumes of the experimental group (Ad-stat1, Ad-stat3-siRNA and Ad-stat1/stat3-siRNA) was smaller than that of the control group, and the difference was significant ($P < 0.05$). The tumor volume of the Ad-stat1/stat3-siRNA dual gene therapy group was smaller than that of the two single gene therapy groups, as shown in Fig. 4A, B. However, the differences are not statistically significant ($P > 0.05$). In addition, we used HE staining to detect the histological changes in tumors derived from different treatment groups. The results found that NCAd-stat1/stat3-siRNA, NCAd-stat1 and NCAd-stat3-siRNA group tumor cells have large and dark nuclei, significantly higher nucleus-cytoplasm

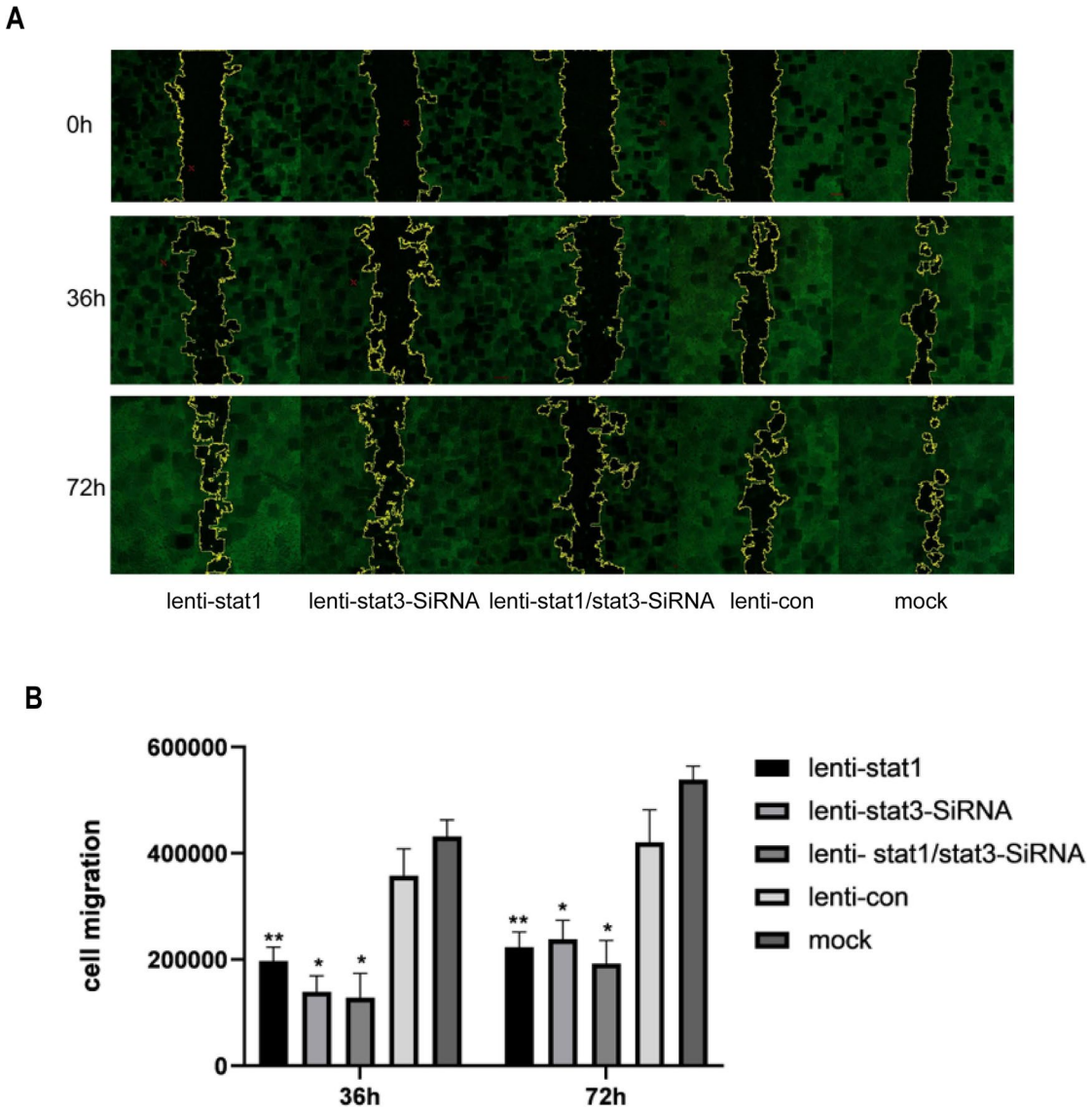

Fig. 3 The effect of various recombinant lentiviruses on the migration of U251 cells. **A** and **B** The migration of U251 cells after infection with lenti-stat1, lenti-stat3-siRNA, and lenti-stat1/stat3-siRNA, lenti-con and mock groups was assessed by Cell scratch assay. Visual fields were taken photo at 0 h 36 h and 72 h. One-way ANOVA was used to analyze intergroup differences with a Bonferroni multiple comparison post-test. n = 3, $^{*}P < 0.05$, $^{**}P < 0.01$

ratio, heterogeneous nuclei, and pathological mitotic phenomena such as meganucleus, dual-nucleus or multi nucleus. (Fig. 5A). The immunohistochemical results are shown in Fig. 5B, C. Compared with the NCAd-stat1/stat3-siRNA, NCAd-stat1, and NCAd-stat3-siRNA group, the STAT1 protein expression levels of the Ad-stat1 group and Ad-stat1/stat3-siRNA group enhanced. The expression levels of STAT3 protein in the Ad-stat3-siRNA group and Ad-stat1/stat3-siRNA group reduced.

In this study, we also used real-time PCR and Western blot methods to detect the expression of STAT1 and STAT3 at the gene and protein levels in tumor tissues. The results showed that compared to control group, the mRNA and protein levels of STAT1 in the Ad-stat1 and Ad-stat1/stat3-siRNA were significantly up-regulated. The mRNA and protein levels of STAT3 were significantly down-regulated in the Ad-stat3-siRNA and the Ad-stat1/stat3-siRNA group, as shown in Fig. 6A, B. We also analyzed the inducing effect of co-expression of Ad-stat1/stat3-siRNA on tumor cell apoptosis in vivo by the TUNEL assays. As shown in Fig. 7, there were almost no apoptotic cell with red fluorescence in NCAd-stat1, NCAd-stat3-siRNA and NCA-stat1/stat3-siRNA groups. Compared to the control group, there were more red fluorescent cells in Ad-stat1, Ad-stat3-siRNA and Ad-stat1/stat3-siRNA groups ($P < 0.05$). The effect of Ad-stat1/stat3-siRNA group was more

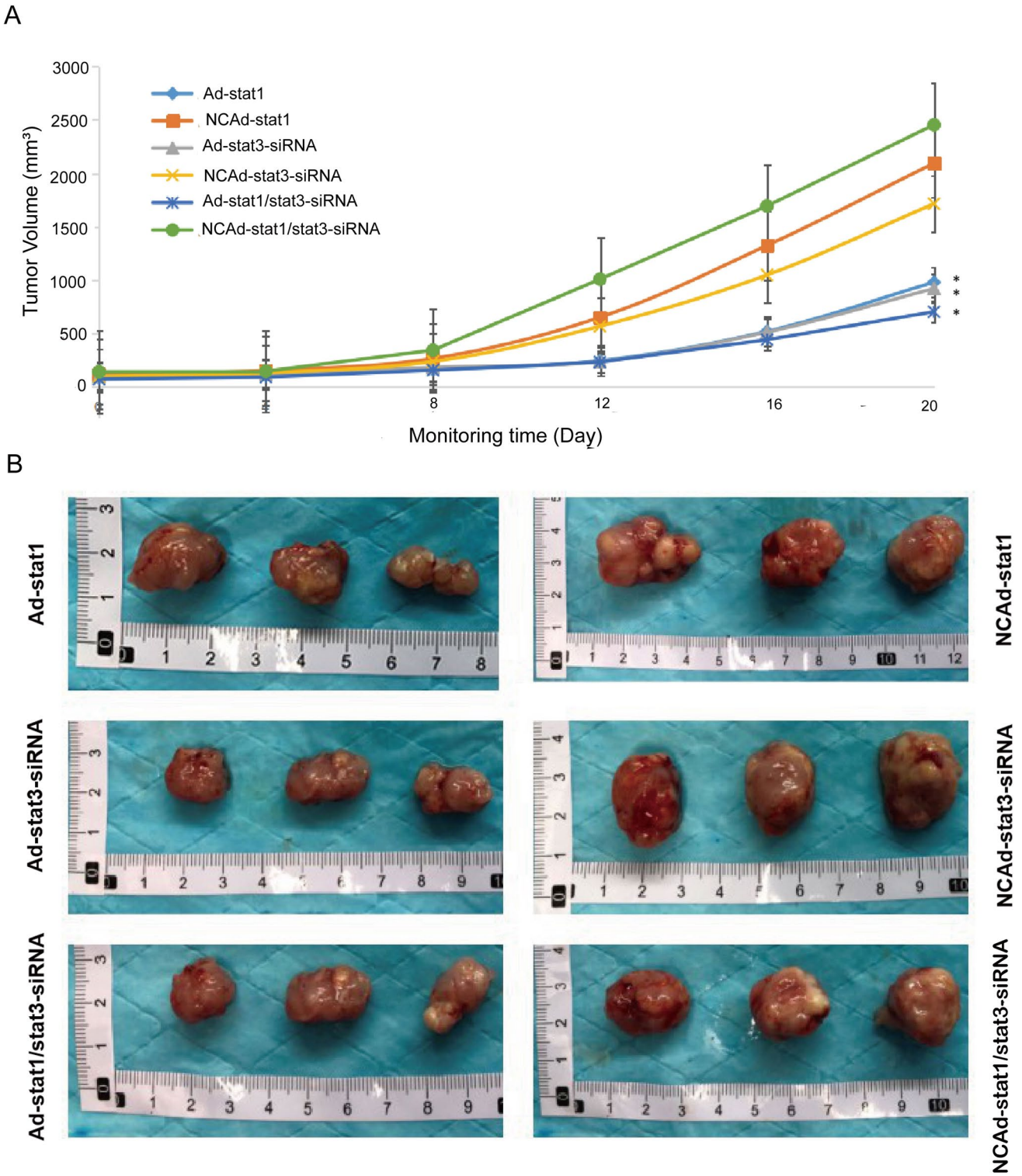

Fig. 4 Effects of recombinant adenovirus Ad-stat1/stat3-siRNA on tumor growth in vivo. Tumors were excised from the nude mice. The long diameter (a) and short diameter (b) of the transplanted tumor were measured before and after the administration. According to the formula ($V = axb^2/2$). **A** Volume and time changes of subcutaneously transplanted tumors of U251 nude mice in each treatment group. The tumor volume-time curve was subsequently plotted. **B** Tumor-bearing status of U251 in nude mice. One-way ANOVA was used to analyze intergroup differences with a Bonferroni multiple comparison post-test. n = 6, * $P < 0.05$ vs related control group

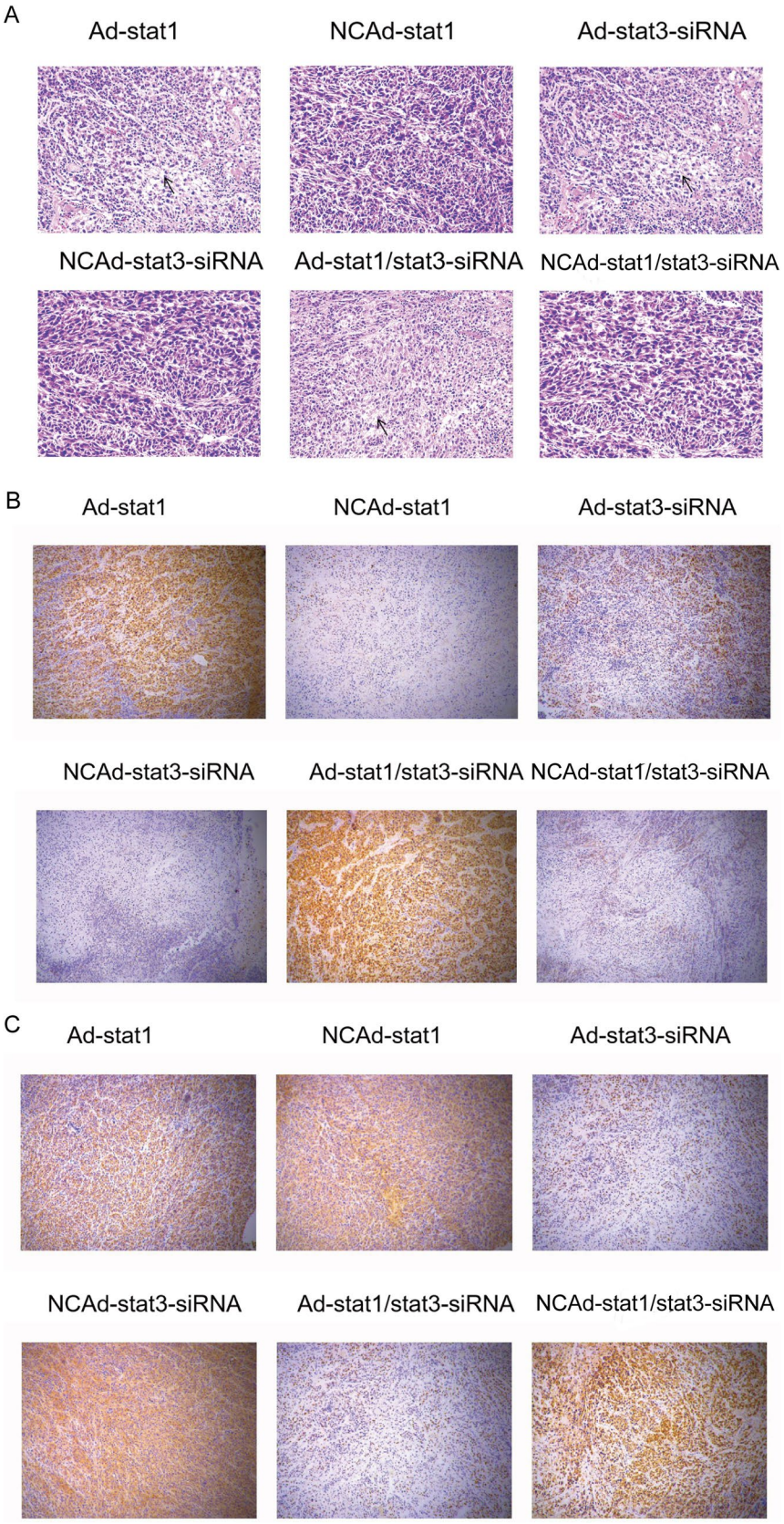

Fig. 5 The in situ expression of stat1 and stat3 in the tumor. **A** HE staining of tumor tissues in each group; **B**, **C** IHC detection of stat1 and stat3 expression in nude mice with U251 xenograft tumor tissue

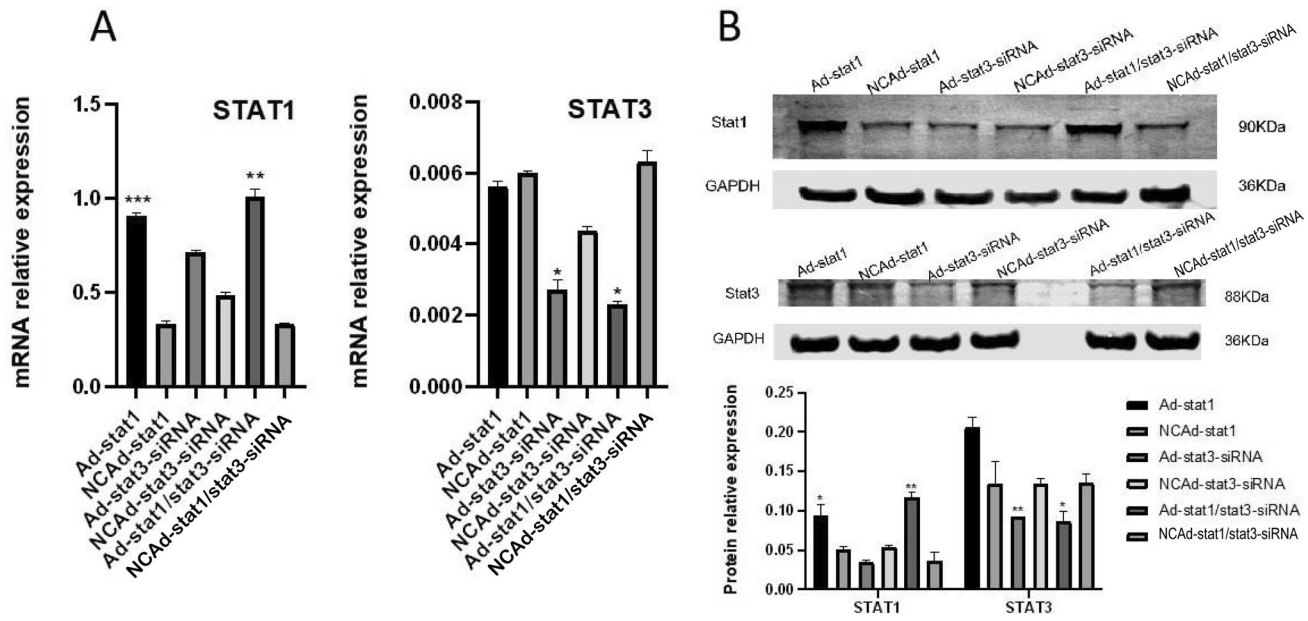

Fig. 6 Stat1 and stat3 mRNA and protein levels in each group tumor tissues. **A** Stat1 and stat3 mRNA levels were determined by qRT-PCR. **B** Stat1 and stat3 protein levels were determined by Western blot. t-test was performed to analyze differences between two groups. n = 6, $^{*}P < 0.05$, $^{**}P < 0.01$, $^{***}P < 0.001$ vs related control group

obvious ($P < 0.05$). The number of apoptotic cells in each group increased significantly compared with the control group.

Analysis of transcriptome sequencing results

To explore the mechanism of the co-expressed genome lenti-stat1/stat3-siRNA compared to single-genome lenti-stat1 or lenti-stat3-siRNA on U251 cell apoptosis, transcriptome sequencing analysis was performed. Differential genes of the three experimental groups were analyzed through Venn diagrams and 936 unique differential genes were identified in the co-expressed genome lenti-stat1/stat3-siRNA (Fig. 8A). These unique differential genes were annotated to the genes expressed by the cell line U251 for KEGG analysis, and the results showed that they were mainly enriched in mineral absorption and FoxO signaling pathway (Fig. 8B). The statistical results $p < 0.05$ showed that BP mainly includes processes such as central nervous system development and multicellular organism processes. CC mainly includes the endoplasmic reticulum, ion channel complexes, etc. MF mainly includes functions such as ion transmembrane transport protein activity and channel regulator activity (Fig. 8C). Additionally, the FOXO signaling pathway is detailed illustrated in Fig. 8D.

Discussion

The pathogenesis of glioma is complex and current treatment methods include surgical resection, postoperative radiotherapy, and chemotherapy. However, most gliomas are infiltrating and diffuse growth, complete removal is challenging, leading to unsatisfactory overall outcomes. Gene therapy has emerged as a promising approach for disease management. While most researches focus on single gene therapy. There is a growing interest in multi-gene combination therapies, which have shown more favorable results. For example, Wang et al. [15] demonstrated that the co-expression of STAT3-specific shRNA and GRIM-19 significantly inhibited tumor cell proliferation, migration, and invasion compared to single-gene approaches, as evidenced by both in vivo and in vitro thyroid cancer treatment. Some scholars have also reported [16] that co-expression of stat3-specific shRNA and GRIM-19 can inhibit the growth and metastasis of prostate cancer more effectively than single gene therapy. In this study, we constructed co-expression plasmids by up-regulating STAT1 and knocking down STAT3, utilizing a viral vector

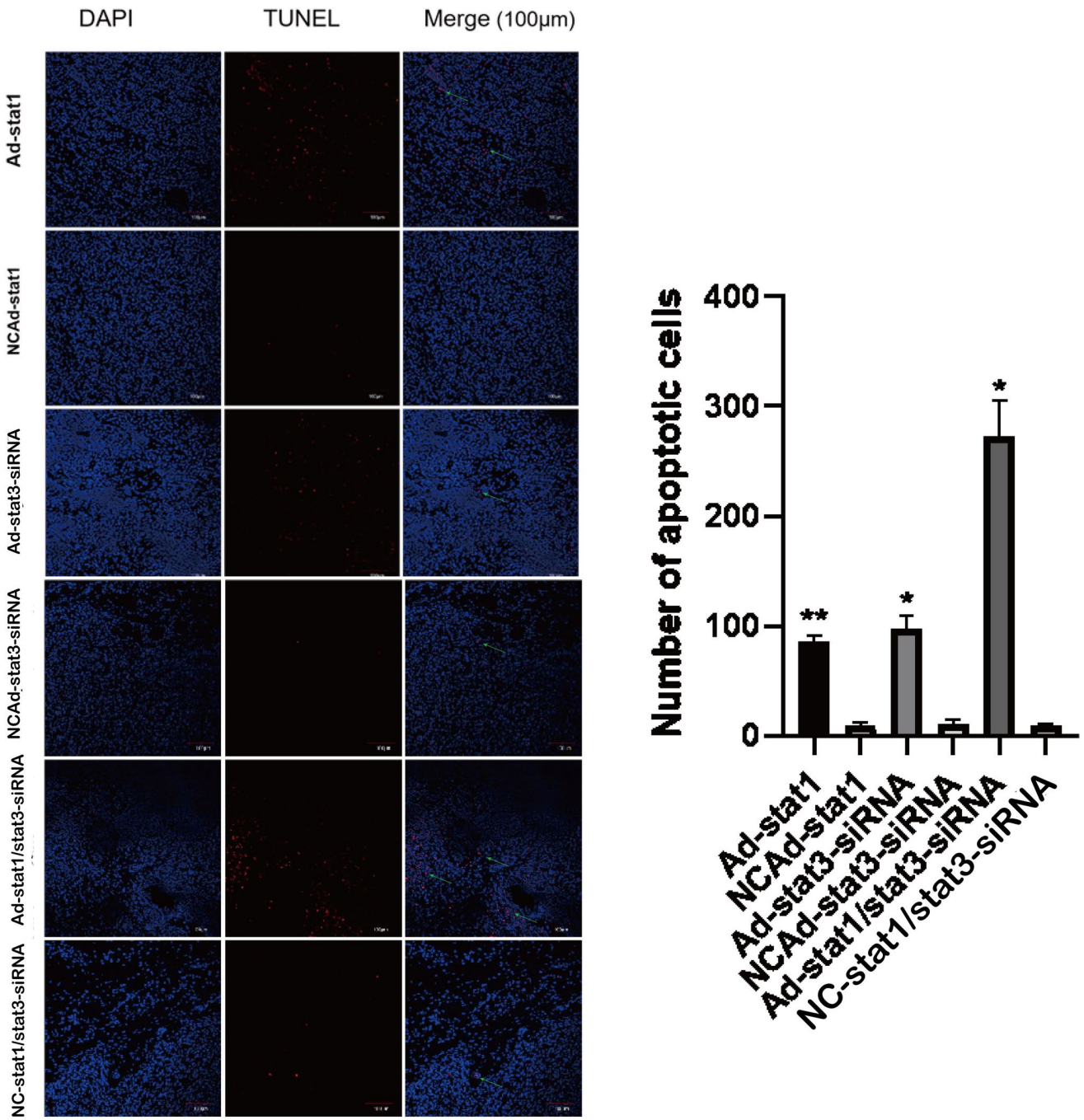

Fig. 7 Effect of co-expression of Ad-stat1/stat3-siRNA on tumor cell apoptosis in vivo. (A-B) Apoptosis was investigated by TUNEL assay. t-test was performed to analyze differences between two groups. n = 6, $^{*}P < 0.05$, $^{**}P < 0.01$ vs related control group

to deliver the target genes directly to the tumor site. Our findings confirm that the infection rates of the viral vector are significantly higher than those of other transfection methods and demonstrated its safety and effectiveness. Our data show that a combined strategy of co-expressed stat1 and stat3-siRNA synergistically and more effectively suppresses glioma growth. In summary, combined gene therapy appears to be more effective in treating cancer than single gene therapy.

To explore the molecular mechanism underlying the effect of co-expression plasmid stat1/stat3-siRNA on glioma cell apoptosis, compared to single gene stat1 and stat3-siRNA, we performed transcriptome sequencing analysis on cell experiments. We analyzed and identified 936

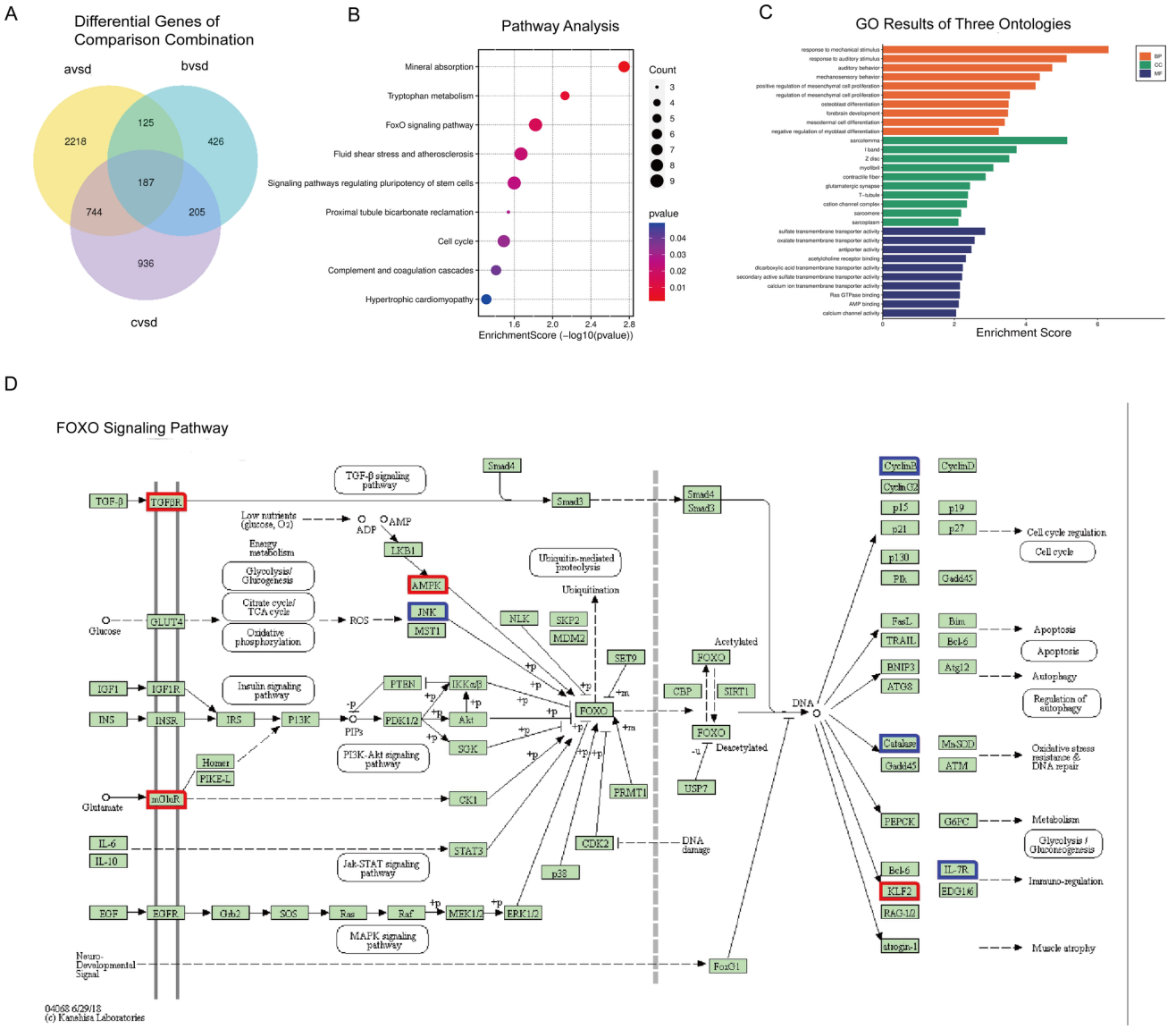

Fig. 8 Analysis of transcriptome sequencing results. The transcriptome was generated using RNA sequencing. Specifically, after extracting total RNA from each group of U251 cells 72 h post-infection with lentivirus, a library was constructed after total RNA sample detection. **A** The Venn diagram of the differential genes of the comparison combination. The sum of all numbers in the circle represents the total number of differential genes in the comparison combination, and the overlapping area represents the number of differential genes shared between the combinations. **B** and **C** KEGG and GO enrichment analysis of 936 unique differential genes in the co-expressed genome lenti-stat1/stat3-siRNA; **D** the diagram of FOXO signaling pathway, Red represents up-regulated genes, and blue represents down-regulated genes

differential genes unique to lenti-stat1/stat3-siRNA through the Venn diagram. Subsequently, we performed GO analysis and Kyoto Encyclopedia of Genes and Genomes (KEGG) pathway analysis on these genes. The KEGG analysis revealed significant enrichment in the mineral absorption and FOXO signaling pathway. FOXO serves as the confluence point of several growth factor receptor tyrosine kinase pathways, with its regulation influenced by main upstream signal pathways, including PI3K-Akt, JAK-STAT, MST1-FOXO, and MAPK signal pathways [17–20]. Some scholars have shown that targeting FOXO1 can effectively induce glioma cell death and inhibit tumor growth. Cheng et al. used curcumin to induce G2/M arrest and trigger apoptosis via FoxO1 signaling in U87 human glioma cells [21, 22]. Additionally, studies have indicated that FoxO3a may play a key role in the differentiation and tumorigenicity control of glioblastoma cancer stem-like cells through PI3K/Akt/mTOR and MEK/ERK signaling pathways [23]. It is known that STAT3 directly affects the FOXO signaling pathway [24]. Notably, when STAT3 is knocked out and STAT1 is

overexpressed, more genes within the FOXO signaling pathway are regulated. TGFBR2, TGFBR3, AMPK, and mGluR are up-regulated, and JNK is down-regulated. The possible mechanism is that the up-regulation of TGFBR2 and TGFBR3 leads to up-regulation of AMPK [25]. AMPK also increases the glycolysis process [26], which in turn reduces oxidative phosphorylation. The decrease in ROS production leads to diminished JNK activities. The above process leads to FOXO phosphorylation regulation that affects the expression levels of downstream genes KLF2, Cyclin B, Catalase, and IL-7R. Of course, FOXO protein and its different phosphorylation modification levels should be assessed. Based on the above results, we speculate that targeting multiple nodes within the FOXO signaling pathway may underpin the enhanced efficacy of the co-expression plasmid stat1/stat3-SiRNA compared to single genome stat1 or stat3-SiRNA in inhibiting the viability and migration of glioma cells. The above results suggest that the anti-glioma effect of overexpressing STAT1 and knocking out STAT3 is not attributable toa single signal pathway. Instead, it appears to be determined by the interplay, whether cooperative or antagonistic, of multiple signaling pathways involving various genes.

There is an interesting result to discuss. Based on the data we could conclude that combined stat1-stat3siRNA improves the apoptotic response of glioma cells when compared to single treatments. In contrast, proliferation, migration and tumor growth are less affected. Glioma is a very complex disease and it is routinely seen that although apoptosis is stimulated, tumor growth may still not be affected. Several limitations need to be acknowledged. Firstly, it is necessary to replicate these results in additional glioma cell lines and an orthotopic model. Secondly, further investigations are need to explore the specific mechanism by which STAT1 overexpression and STAT3 silencing on glioma.

Conclusion

Co-expression of plasmid stat1/stat3-siRNA can significantly increase the expression of stat1 gene and inhibit the expression of stat3 gene in glioma cells. The co-expression plasmid demonstrates a more pronounced ability to induce apoptosis compared to the single genome stat1 and stat3-siRNA. RNA sequencing analysis indicated that multiple genes of the FOXO signaling pathway are altered by co-expression plasmid stat1/stat3-siRNA, which may contribute to its superior effectiveness in inducing apoptosis compared to single-gene therapies. Further investigation into the underlying mechanisms is warranted.

Supplementary Information The online version contains supplementary material available at https://doi.org/10.1007/s11033-025-10585-1.

Acknowledgements The authors are grateful to the Molecular Pathology Laboratory of Inner Mongolia Agricultural University for their help and support for this experiment.

Author contributions Haitao Ju and Changwu Dou designed the study. Xinlong Hu、Hong Li and Guodong Zhang performed the experiments and analyzed the data. Xinlong Hu wrote the manuscript. Chao Lin, Ping Huang, Xiufeng Chen and Fang Wan critically revised the article. All authors read and approved the final manuscript.

Funding This work was funded by the national Natural Science Foundation of China (Nos. 8166110006) and the Great Natural Science Foundation of Affiliated Hospital of Inner Mongolia Medical University (Nos. NYFYZD2014009, 2019LH08029,YKDX2021LH003 and YKD2022TD029).

Data availability No datasets were generated or analysed during the current study.

Declarations

Competing interests The authors declare no competing interests.

Ethical approval This study has been approved by the Medical Ethics Committee of Inner Mongolia Medical University (YKD2015068). All methods were performed in accordance with the relevant guidelines and regulations.

References

1. Grochans S, Cybulska AM, Simińska D, Korbecki J, Kojder K, Chlubek D, Baranowska-Bosiacka I (2022) Epidemiology of glioblastoma multiforme-literature review. Cancers 14(10):2412. https://doi.org/10.3390/cancers14102412
2. Bender E (2016) Gene therapy: industrial strength. Nature 537(7619):S57–S59. https://doi.org/10.1038/537S57a
3. Kurozumi K, Koizumi S, Otani Y (2021) No Shinkei Geka. Neurol Surg 49(3):608–616. https://doi.org/10.11477/mf.1436204434
4. Philips RL, Wang Y, Cheon H, Kanno Y, Gadina M, Sartorelli V, Horvath CM, Darnell JE Jr, Stark GR, O'Shea JJ (2022) The JAK-STAT pathway at 30: much learned, much more to do. Cell 185(21):3857–3876. https://doi.org/10.1016/j.cell.2022.09.023
5. Ou A, Ott M, Fang D, Heimberger AB (2021) The Role and therapeutic targeting of JAK/STAT signaling in glioblastoma. Cancers 13(3):437. https://doi.org/10.3390/cancers13030437

6. Li YJ, Zhang C, Martincuks A, Herrmann A, Yu H (2023) STAT proteins in cancer: orchestration of metabolism. Nat Rev Cancer 23(3):115–134. https://doi.org/10.1038/s41568-022-00537-3
7. Ji W, Liu Y, Xu B, Mei J, Cheng C, Xiao Y, Yang K, Huang W, Jiao J, Liu H, Shao J (2021) Bioinformatics analysis of expression profiles and prognostic values of the signal transducer and activator of transcription family genes in glioma. Front Genet 12:625234. https://doi.org/10.3389/fgene.2021.625234
8. Swiatek-Machado K, Kaminska B (2020) STAT signaling in glioma cells. Adv Exp Med Biol 1202:203–222. https://doi.org/10.1007/978-3-030-30651-9_10
9. Kulesza DW, Przanowski P, Kaminska B (2019) Knockdown of STAT3 targets a subpopulation of invasive melanoma stem-like cells. Cell Biol Int 43(6):613–622. https://doi.org/10.1002/cbin.11134
10. Ju H, Li X, Li H, Wang X, Wang H, Li Y, Dou C, Zhao G (2013) Mediation of multiple pathways regulating cell proliferation, migration, and apoptosis in the human malignant glioma cell line U87MG via unphosphorylated STAT1: laboratory investigation. J Neurosurg 118(6):1239–1247. https://doi.org/10.3171/2013.3.JNS122051
11. Han D, Yu T, Dong N, Wang B, Sun F, Jiang D (2019) Napabucasin, a novel STAT3 inhibitor suppresses proliferation, invasion and stemness of glioblastoma cells. J Exp Clin Cancer Res 38(1):289. https://doi.org/10.1186/s13046-019-1289-6
12. Shen Y, Thng DKH, Wong ALA, Toh TB (2024) Mechanistic insights and the clinical prospects of targeted therapies for glioblastoma: a comprehensive review. Exp Hematol Oncol 13(1):40. https://doi.org/10.1186/s40164-024-00512-8
13. Lin Y, He Z, Ye J, Liu Z, She X, Gao X, Liang R (2020) Pro gress in understanding the IL-6/STAT3 pathway in colorectal cancer. Onco Targets Ther 13:13023–13032. https://doi.org/10.2147/OTT.S278013
14. Kim BH, Lee H, Park CG, Jeong AJ, Lee SH, Noh KH, Park JB, Lee CG, Paek SH, Kim H, Ye SK (2020) Stat3 inhibitor odz10117 suppresses glioblastoma malignancy and prolongs survival in a glioblastoma xenograft model. Cells. https://doi.org/10.3390/cells9030722
15. Wang GM, Ren ZX, Wang PS, Su C, Zhang WX, Liu ZG, Zhang L, Zhao XJ, Chen G (2014) Plasmid-based Stat3-specific siRNA and GRIM-19 inhibit the growth of thyroid cancer cells in vitro and in vivo. Oncol Rep 32(2):573–580. https://doi.org/10.3892/or.2014.3233
16. Zhang L, Gao L, Li Y, Lin G, Shao Y, Ji K, Yu H, Hu J, Kalvakolanu DV, Kopecko DJ, Zhao X, Xu DQ (2008) Effects of plasmid-based Stat3-specific short hairpin RNA and GRIM-19 on PC-3M tumor cell growth. Clin Cancer Res 14(2):559–568. https://doi.org/10.1158/1078-0432.CCR-07-1176
17. Orea-Soufi A, Paik J, Bragança J, Donlon TA, Willcox BJ, Link W (2022) FOXO transcription factors as therapeutic targets in human diseases. Trends Pharmacol Sci 43(12):1070–1084. https://doi.org/10.1016/j.tips.2022.09.010
18. Farhan M, Wang H, Gaur U, Little PJ, Xu J, Zheng W (2017) FOXO signaling pathways as therapeutic targets in cancer. Int J Biol Sci 13(7):815–827. https://doi.org/10.7150/ijbs.20052
19. Liu Y, Ao X, Jia Y, Li X, Wang Y, Wang J (2022) The FOXO family of transcription factors: key molecular players in gastric cancer. J Mol Med (Berl) 100(7):997–1015. https://doi.org/10.1007/s00109-022-02219-x
20. Greer EL, Oskoui PR, Banko MR, Maniar JM, Gygi MP, Gygi SP, Brunet A (2007) The energy sensor AMP-activated protein kinase directly regulates the mammalian FOXO3 transcription factor. J Biol Chem 282(41):30107–30119. https://doi.org/10.1074/jbc.M705325200
21. Lau CJ, Koty Z, Nalbantoglu J (2009) Differential response of glioma cells to FOXO1-directed therapy. Can Res 69(13):5433–5440. https://doi.org/10.1158/0008-5472.CAN-08-4540
22. Cheng C, Jiao JT, Qian Y, Guo XY, Huang J, Dai MC, Zhang L, Ding XP, Zong D, Shao JF (2016) Curcumin induces G2/M arrest and triggers apoptosis via FoxO1 signaling in U87 human glioma cells. Mol Med Rep 13(5):3763–3770. https://doi.org/10.3892/mmr.2016.5037
23. Sunayama J, Sato A, Matsuda K, Tachibana K, Watanabe E, Seino S, Suzuki K, Narita Y, Shibui S, Sakurada K, Kayama T, Tomiyama A, Kitanaka C (2011) FoxO3a functions as a key integrator of cellular signals that control glioblastoma stem-like cell differentiation and tumorigenicity. Stem Cells (Dayton, Ohio) 29(9):1327–1337. https://doi.org/10.1002/stem.696
24. Li Y, Jiang F, Zhu S, Jia H, Li C (2024) STAT3 drives the malignant progression of low-grade gliomas through modulating the expression of STAT1, FOXO1, and MYC. Front Mol Biosci 11:1419072. https://doi.org/10.3389/fmolb.2024.1419072
25. Rios Garcia M, Steinbauer B, Srivastava K, Singhal M, Mattijssen F, Maida A, Christian S, Hess-Stumpp H, Augustin HG, Müller-Decker K, Nawroth PP, Herzig S, Berriel Diaz M (2017) Acetyl-CoA carboxylase 1-dependent protein acetylation controls breast cancer metastasis and recurrence. Cell Metab 26(6):842-855.e5. https://doi.org/10.1016/j.cmet.2017.09.018
26. Chaube B, Bhat MK (2016) AMPK, a key regulator of metabolic/energy homeostasis and mitochondrial biogenesis in cancer cells. Cell Death Dis 7(1):e2044. https://doi.org/10.1038/cddis.2015.404